

Characterization of Biaxial Mechanical Behavior of Porcine Aorta under Gradual Elastin Degradation

SHAHROKH ZEINALI-DAVARANI,¹ MING-JAY CHOW,¹ RAPHAËL TURCOTTE,^{2,3} and YANHANG ZHANG^{1,2}

¹Department of Mechanical Engineering, Boston University, 110 Cummington Mall, Boston, MA 02215, USA; ²Department of Biomedical Engineering, Boston University, 44 Cummington Mall, Boston, MA 02215, USA; and ³Advanced Microscopy Program, Center for Systems Biology and Wellman Center for Photomedicine, Massachusetts General Hospital, Harvard Medical School, Boston, MA 02114, USA

(Received 14 August 2012; accepted 19 December 2012)

Associate Editor Ender A. Finol oversaw the review of this article.

Abstract—Arteries are composed of multiple constituents that endow the wall with proper structure and function. Many vascular diseases are associated with prominent mechanical and biological alterations in the wall constituents. In this study, planar biaxial tensile test data of elastase-treated porcine aortic tissue (Chow *et al.* in *Biomech Model Mechanobiol* 2013) is re-examined to characterize the altered mechanical behavior at multiple stages of digestion through constitutive modeling. Exponential-based as well as recruitment-based strain energy functions are employed and the associated constitutive parameters for individual digestion stages are identified using nonlinear parameter estimation. It is shown that when the major portion of elastin is degraded from a cut-open artery in the load-free state, the embedded collagen fibers are recruited at lower stretch levels under biaxial loads, leading to a rapid stiffening behavior of the tissue. Multiphoton microscopy illustrates that the collagen waviness decreases significantly with the degradation time, resulting in a rapid recruitment when the tissue is loaded. It is concluded that even when residual stresses are released, there exists an intrinsic mechanical interaction between arterial elastin and collagen that determines the mechanics of arteries and carries important implications to vascular mechanobiology.

Keywords—Aneurysms, Elastin degradation, Vascular mechanics, Recruitment distribution function, Multiphoton microscopy, Collagen waviness.

INTRODUCTION

The arterial wall is a complex combination of multiple structurally significant components such as elastin, collagen fibers, and smooth muscle cells. Together,

these constituents determine the mechanical response of the arterial wall. The passive mechanical behavior of arteries is believed to be mainly dominated by elastin in the toe region of the stress–strain response where collagen fibers are undulated. Collagen fibers are progressively recruited and dominate the wall mechanical response at higher stretch levels.^{17,23,28} Changes in the mechanical behavior of the wall in vascular diseases are associated with alterations in its structure. For instance, decrease in elastin content, disruption of elastin network, as well as elevated collagen content^{7,8,20,40} are common features of Abdominal Aortic Aneurysms (AAAs). These structural changes are associated with a remarkable increase in stiffness of the AAA wall.^{31,50,52} Elastin degradation is thought to contribute to the growth of aneurysms early on, whereas rupture of the lesion is attributed to the loss of collagen integrity.¹¹ Changes in the mechanical response and ultimately failure of the AAA wall are suggested to be the result of defects in the collagen network, rather than defects at the molecular level.³⁵

Prior to focusing on the critical role of mechanobiology in the development and the progression of AAAs, we need to improve our knowledge of the aortic wall mechanics as it not only drives the arterial AAAs growth and remodeling³⁰ but also determines the failure of the tissue through wall stress or strain.⁵³ Therefore, the sequences of structural alterations and the resulting mechanical responses due to elastin degradation are particularly important. The roles of elastin and collagen in arterial mechanics are suggested to be highly coupled and interactive.^{9,10,13,15} Chow *et al.*⁹ recently conducted *in vitro* degradation of elastin in order to study the resulting progressive changes in the arterial structure and mechanical behavior. Elastin and collagen assays

Address correspondence to Yanhang Zhang, Department of Mechanical Engineering, Boston University, 110 Cummington Mall, Boston, MA 02215, USA. Electronic mail: yanhang@bu.edu

were performed to quantify biochemical changes in the extracellular matrix while histological assessments revealed gradual changes in the microstructure and planar biaxial tensile tests showed progressive changes in the mechanical response due to elastin degradation.

Continuum mechanics theory has been widely used to describe arterial mechanics with a variety of strain energy functions (see reviews by Holzapfel *et al.*^{23,24}, Humphrey²⁹). In this study, we use multiple constitutive relations to describe the mechanical responses of digested aortic tissues in planar biaxial tensile tests⁹ and to relate the gradual changes in the mechanical response with the structural alterations. In doing so, we choose representative exponential-based as well as recruitment-based strain energy functions to model the observed changes in the mechanical response. Multi-photon microscopy is used to observe the underlying microstructural changes as a result of elastin digestion.

MATERIALS AND METHODS

Sample Preparation, Chemical Degradation and Mechanical Testing

The experimental procedure of elastin degradation and the mechanical testing are described in detail by Chow *et al.*⁹ Briefly, a total of 60 porcine thoracic aortas from 12 to 24 month old pigs are cut into square samples ($\sim 1.5 \times 1.5$ cm) and divided into five groups undergoing various digestion times (6, 12, 24, 48, and 96 h of digestion; 12 samples for each group). A 5 U/mL ultra-pure elastase solution (MP Biomedicals, Solon, OH) is used to degrade tissues at 37 °C with gentle stirring. A custom designed biaxial tensile testing device is used to characterize the planar biaxial mechanical behavior of the fresh and digested samples. Samples are preconditioned through 8 loading cycles up to 30 N/m. Following the preconditioning cycles, a preload of 2 ± 0.050 N/m is applied in order to keep sutures straightened. The preloaded configuration is chosen as the reference configuration for stress and stretch calculations. Eight cycles of equi-biaxial tension are applied to capture the stress–stretch responses. The maximum stress in the samples generally exceeds 100 kPa and is chosen to obtain as much data from the physiologically relevant pressure range without irreversibly damaging the tissue. The mechanical test data of the 12 samples in each group are then averaged and used as the representative behavior of that time group for the constitutive modeling.

Constitutive Modeling

To describe the biaxial mechanical behavior of samples using constitutive models, the corresponding

strain energy functions are decomposed into two additive parts, i.e., $W = W_e + W_c$.²⁴ The elastin-dominated ground substance is represented by a neo-Hookean form of the strain energy function, $W_e = c_e/2(I_1 - 3)$ where c_e is a parameter associated with elastin and $I_1 = \text{tr}(\mathbf{C})$ the first invariant of the right Cauchy-Green deformation tensor \mathbf{C} .^{26,27,56} Based on previous literature, an exponential-based as well as two recruitment-based strain energy functions representing collagen fibers are chosen as:

Model A

Motivated by Fung,¹⁶ Holzapfel *et al.*²³ proposed a multi-layer fiber-reinforced composite model for the arterial wall that considers the histological structure of arteries along with an exponential form that represents the prominent stiffening characteristics of the arterial collagen. Assuming one-layer and multiple families of collagen fibers, we use:^{4,14,57,58}

$$W_c = \sum_{k=1}^N \frac{c_1^{(k)}}{N c_2^{(k)}} \left[\exp \left\{ c_2^{(k)} (\lambda_k^2 - 1)^2 \right\} - 1 \right] \quad (1)$$

$$\text{where } \lambda_k = \sqrt{(\lambda_\theta \sin \alpha_k)^2 + (\lambda_Z \cos \alpha_k)^2}$$

In Eq. (1) λ_k , $c_1^{(k)}$, and $c_2^{(k)}$ are the stretch and constitutive parameters associated with the fiber family k oriented with an angle of α_k with respect to the longitudinal direction. N is the total number of fiber families chosen to be two (two diagonal fiber families with equal mechanical properties, i.e., $c_1^{(1)} = c_1^{(2)}$ and $c_2^{(1)} = c_2^{(2)}$, and symmetric orientations with respect to the longitudinal direction, i.e., $\alpha_1 = -\alpha_2 = \alpha$) or four (four-fiber-family model considering two additional fiber families in longitudinal and circumferential directions, i.e., $\alpha_3 = 0^\circ$ and $\alpha_4 = 90^\circ$).

Model B

Collagen fibers embedded in tissues naturally have an undulated structure. Each fiber becomes straight and engages in load bearing at a different level of stretch (i.e., recruitment stretch) depending on its degree of waviness. Zulliger *et al.*⁶⁰ proposed a two-fiber-family model that considers a log-logistic statistical distribution for the recruitment of fibers. The total strain energy stored in two families of fibers can be expressed by:

$$W_c = \sum_{k=1}^2 \frac{1}{2} \psi_f * \rho_f = \sum_{k=1}^2 \frac{1}{2} \int_{-\infty}^{\infty} \psi_f(E_k - x) \rho_f(x) dx \quad (2)$$

where $E_k = 1/2(\lambda_k^2 - 1)$ is the strain in the direction of fiber families. Individual collagen fibers are assumed to

behave linearly, i.e., $\psi_f(E_k) = 1/2c_c E_k^2$ ⁴⁴ and engage with a log-logistic probability distribution as

$$\rho_f(E_k) = \begin{cases} \frac{a_k}{b_k} \frac{\left(\frac{E_k}{b_k}\right)^{a_k-1}}{\left[1 + \left(\frac{E_k}{b_k}\right)^{a_k}\right]^2} & E_k < 0 \\ 0 & E_k \leq 0 \end{cases} \quad (3)$$

where $c_c = 200$ MPa, an elastic constant stemming from intrinsic properties of collagen fibers.^{15,44,60} $a_k > 0$ and $b_k > 0$ are parameters that determine the shape of the engagement distribution of fiber family k . Smaller b_k induces engagement at lower stretch levels while smaller a_k results in a more spread out (slower) engagement of fibers. Two symmetric diagonal fiber families are considered to have equal properties of engagement ($a_1 = a_2$ and $b_1 = b_2$).

Model C

Lanir³³ presented a structural model for the biaxial stress-strain response of collagenous tissues considering non-uniform angular as well as waviness distributions of fibers. A normal statistical distribution was suggested for the recruitment stretch as:

$$\rho_f(E_k) = \frac{1}{d_k \sqrt{2\pi}} \exp\left(-\frac{(E_k - m_k)^2}{2d_k^2}\right) \quad (4)$$

where $m_k > 0$ and $d_k > 0$ represent the mean and standard deviation of the normal distribution, defining the shape of the engagement distribution. The normal distribution is incorporated into the Eq. (2) two families of diagonal fibers with equal properties of engagement ($m_1 = m_2$ and $d_1 = d_2$).

Given the strain energy functions, the Cauchy stress can be calculated as:^{22,28}

$$\mathbf{T} = -p\mathbf{I} + \mathbf{F} \frac{\partial W}{\partial \mathbf{C}} \mathbf{F}^T \quad (5)$$

where \mathbf{F} is the deformation gradient and p is a Lagrange multiplier obtained using the incompressibility and plane stress assumptions.

Parameter Estimation

Parameters associated with each constitutive relation are estimated separately by minimizing the difference between the calculated stress from the constitutive relations, T^c and the stress obtained from the biaxial tests,⁹ T^e , in the form of an objective function as

$$S = \sum_{i=1}^n \left\{ w_1 (T_{11}^c - T_{11}^e)_i^2 + w_2 (T_{22}^c - T_{22}^e)_i^2 \right\} \quad (6)$$

where n is the sample size and subscripts 1 and 2 correspond to the longitudinal and circumferential direc-

tions. w_1 and w_2 are constant weight parameters. A direct search method, built in Matlab Optimization Toolbox, is employed to minimize the objective function with appropriate constraints on the constitutive parameters. As a measure of the goodness-of-fit, a root-mean-square (RMS) measure of error is calculated as⁵⁵

$$\text{RMS} = \sqrt{\frac{\sum_1^n (T_{11}^c - T_{11}^e)^2}{n}} + \sqrt{\frac{\sum_1^n (T_{22}^c - T_{22}^e)^2}{n}} \quad (7)$$

Multiphoton Microscopy

A mode-locked Ti:sapphire laser (Maitai-HP, wavelength 800 nm, 100 fs pulse width, 80 MHz repetition rate, Spectra-Physics) is used to generate second-harmonic generation (SHG) from collagen at 400 nm (417/80 nm) and two-photon excitation autofluorescence from elastin at 525 nm (525/45 nm). An average power of 25 mW is delivered to the sample. Image acquisition is performed on a multiphoton video-rate microscope⁵¹ over a 1 cm² area by systematic random sampling (3.24% of the surface area⁴¹) on both the adventitia and the intima side. At each location, a 3D volume is recorded over a depth of 60 μm and with a field of view of 360 μm . A quarter-wave plate is placed just before the objective (60X, NA1.0W, LUMPlanN, Olympus) to generate a quasi-circular polarization (1.8 dB) in order to alleviate the excitation polarization dependence of the SHG. For the assessment of collagen fiber reorganization upon chemical degradation, the imaging experiment is repeated with multiple fresh and digested (6, 12, 24 and 48 h) planar samples that were not fixed or loaded.

Quantification of Waviness for Collagen Fibers

The waviness of collagen fibers is quantified for a subset of adventitial images at different stages of digestion using NeuronJ (a plug-in of ImageJ). NeuronJ, originally developed for neuron tracing,^{38,39} has been successfully used for analysis of the adventitial collagen by Rezakhaniha *et al.*⁴³ Given the Euclidean distance between the end points of a fiber bundle (L) as well as the fiber length (l) by the software, the straightness parameter ($P_s = L/l$) is calculated to measure the degree of waviness. The larger the P_s , the more straight the fiber. $P_s = 1$ indicates a completely straight fiber.

Statistical Analysis

The straightness parameters and elastin contents at various digestion time points are compared using a factorial analysis of variance. A two-tailed $p < 0.05$ is considered statistically significant with post hoc testing

using the Tukey's method to adjust for multiple comparisons. Statistical analysis is performed using the JMP statistical package (version 9.0.2, 2010 SAS Institute Inc.).

RESULTS

Analyses of histology as well as elastin and collagen biological assays at different stages of digestion have been elaborated by Chow *et al.*⁹ Figure 1 shows the stress-stretch data in longitudinal and circumferential directions averaged between all samples in each time group (i.e., 12 samples). Due to the gradual elastin digestion the stress-strain response exhibits an initial softening followed by an S-shaped elastomer-like response which eventually turns into a stiff collagen scaffold response (see Chow *et al.*⁹ for more details). The fitted curves using Model A assuming two diagonal fiber families are also overlaid in Fig. 1. The estimated parameters associated with each time groups are shown in Table 1. The estimated parameter for collagen, c_2^i , is much larger at 24, 48, and 96 h digestion time steps compared to the initial stages of digestion. Lower values for the ratio of c_1^i/c_2^i in these stages of degradation also imply more contribution of collagen fibers to the stored energy.^{10,14} An initial increase, followed by a decreasing trend in c_e can be noticed, contrary to the notion that the contribution of elastin is consistently reducing due to degradation. In Table 2 parameters associated with Model A considering four families of collagen fibers are presented. Fitted curves are not shown as there is no considerable difference in the quality of fit between 2-fiber-family and 4-fiber-family models in this study which can be noticed from the fairly close values of RMS error in Tables 1 and 2. A similar trend in the material parameters can be observed in the diagonal directions ($i = 3, 4$) with digestion, implying a stiffer response for a highly digested arterial tissue.

Estimated parameters associated with Model B are given in Table 3. Elastin parameter, c_e , consistently decreases with the digestion time suggesting a diminishing contribution of elastin to the strain energy in the biaxial deformation. Smaller values of b_k and larger values for a_k estimated in the advanced stages of degradation (24, 48, 96 h) indicate earlier engagement of collagen fibers with a narrower distribution. Table 4 presents the parameters estimated for Model C. Both the mean value, m , and the standard deviation, d , of the recruitment distribution show an overall decreasing trend with the digestion time while the contribution of elastin to the strain energy (i.e., reduction in the parameter c_e) continuously drops.

Figure 2 illustrates the resulting recruitment distribution density functions using the estimated

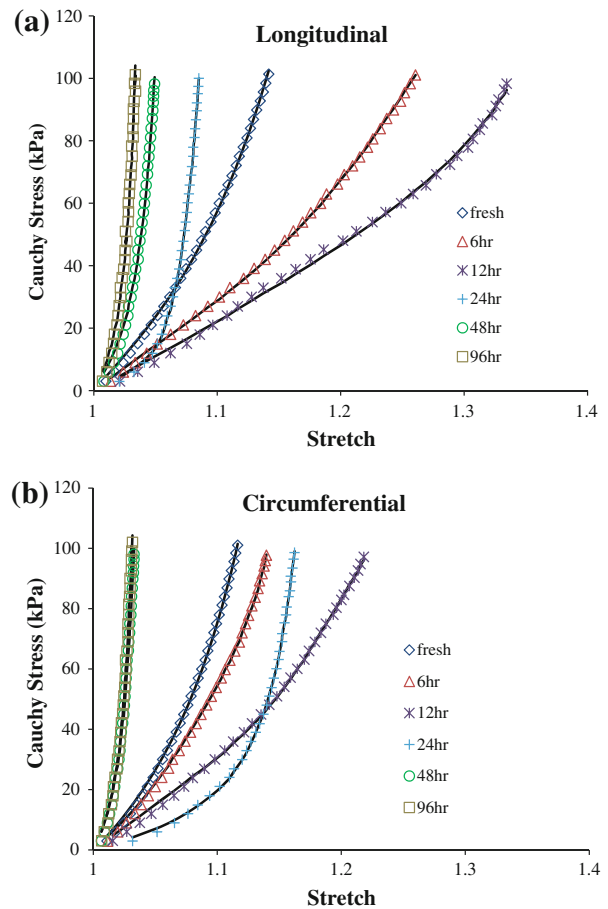


FIGURE 1. Cauchy stress vs. stretch plots of the biaxial tensile test data (symbols) as well as the fitted curves (lines) using the estimated parameters of Model A in (a) longitudinal and (b) circumferential directions for multiple digestion time steps.

parameters for Models B and C. Recruitments of fibers peaks earlier at 24, 48 and 96 h stages compared to the recruitments at the initial stages (fresh, 6, and 12 h) which appear to be relatively negligible within the same range of strain. Although the peak values (sharpness) of distributions at the advanced stages are apparently higher than the initial stages, they do not show consistent trend within themselves. It should be noted that the time to peak (determined by parameters b_k, m_k) together with the peak value of distribution (determined by parameters a_k, d_k) both relate to the structure of fibers (waviness) and are not inherently independent parameters.

Figure 3a shows a representative image of collagen (blue) and elastin (green) recorded simultaneously from the intima side of a fresh sample using multi-photon microscopy. The image is then split into separate images of collagen (Fig. 3b) and elastin (Fig. 3c). After 6 h of digestion no elastin network appears in our microscopic images from either the adventitia or the intima side due to scanning depth limitations of the

TABLE 1. Estimated parameters using Model A assuming two symmetric collagen fiber families.

	Fresh	6 h	12 h	24 h	48 h	96 h
$c_1^1 = c_1^2$ (kPa)	211.0	81.9	35.6	29.8	382.0	424.0
$c_2^1 = c_2^2$	4.27	2.07	1.35	33.9	151.0	283.0
c_e (kPa)	7.12×10^{-14}	28.9	31.3	15.4	6.03×10^{-12}	4.56×10^{-12}
α (°)	45.5	48.9	49.9	42.5	45.4	45.1
RMS	1.86×10^3	1.36×10^3	2.21×10^3	1.30×10^3	3.55×10^3	4.28×10^3

TABLE 2. Estimated parameters using Model A assuming four collagen fiber families.

	Fresh	6 h	12 h	24 h	48 h	96 h
c_1^1 (kPa)	72.1	29.4	2.06×10^{-24}	2.77×10^{-12}	5.53×10^{-26}	1.92×10^{-14}
c_2^1 (kPa)	1.22×10^{-9}	1.01×10^{-12}	1.89×10^{-13}	7.89×10^{-14}	1.14×10^{-11}	6.95×10^{-12}
$c_3^1 = c_1^4$ (kPa)	175.0	82.6	35.6	29.8	382.0	424.0
c_2^2	1.64	4.60×10^{-13}	3.45×10^{-11}	0.158	1.36×10^{-12}	1.23×10^{-3}
$c_3^2 = c_2^4$	4.82×10^{-11}	2.00×10^{-18}	1.75×10^{-21}	1.13×10^{-18}	5.30×10^{-14}	0.0152
$c_4^2 = c_2^4$	4.96	2.24	1.35	33.9	151.0	283.0
c_e (kPa)	5.35×10^{-13}	21.5	31.3	15.4	1.97×10^{-19}	2.51×10^{-13}
α (°)	51.3	54.9	49.9	42.5	45.4	45.1
RMS	1.75×10^3	1.11×10^3	2.21×10^3	1.30×10^3	3.55×10^3	4.28×10^3

TABLE 3. Estimated parameters using Model B assuming two collagen fiber families.

	Fresh	6 h	12 h	24 h	48 h	96 h
$a_1 = a_2$	1.01	0.948	1.11	4.70	1.39	1.65
$b_1 = b_2$	31.8	138.0	126.0	0.308	0.558	0.234
c_e (kPa)	55.4	47.4	39.8	32.6	1.50×10^{-11}	3.35×10^{-17}
α (°)	46.3	51.2	51.7	41.6	45.4	45.0
RMS	7.28×10^2	1.47×10^3	2.52×10^3	2.48×10^3	2.37×10^3	4.16×10^3

TABLE 4. Estimated parameters using Model C assuming two collagen fiber families.

	Fresh	6 h	12 h	24 h	48 h	96 h
$d_1 = d_2$	2.99	2.42	1.17	0.0636	0.0710	0.0380
$m_1 = m_2$	5.21	5.80	3.60	0.264	0.169	0.0970
c_e (kPa)	56.1	49.6	40.8	28.5	3.17×10^{-11}	6.30×10^{-17}
α (°)	46.3	51.6	51.9	41.8	45.4	45.1
RMS	7.22×10^2	1.46×10^3	2.45×10^3	2.02×10^3	1.68×10^3	3.48×10^3

multiphoton microscope. Representative images of collagen fibers captured from both adventitia and intima sides of fresh and digested samples are depicted in Fig. 4. Undulated bundles of collagen can be seen in the fresh sample as well as 6 and 12 h digestion stages from both sides. As the degradation proceeds (after 24 h), collagen fibers straighten out and turn into straight bundles of fibers. Figure 5 further illustrates multiple families of straight collagen fibers in the adventitia of a sample after 48 h of digestion at various scanning depths (6 μ m spacing).

Figure 6 presents the measured waviness of the adventitial collagen obtained from SHG images at different stages of elastin degradation. The increasing trend in the straightness parameter indicates reduced waviness of collagen as a result of elastin digestion. Analysis of variance reveals that collagen fibers are significantly more undulated at the fresh stage compared to the other stages and fibers become straighter with longer digestion time. While there is no significant difference in the waviness between 6 and 12 h ($p = 0.7423$) as well as between 24 and 48 h ($p = 1$),

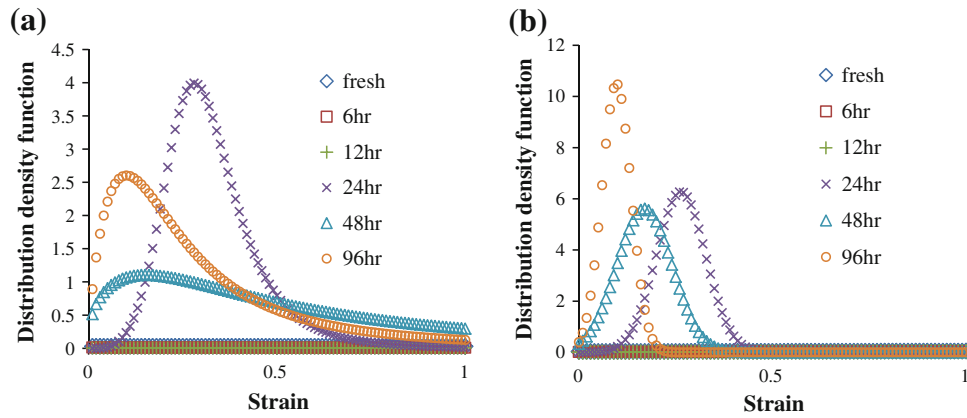


FIGURE 2. Distribution density functions vs. strain in the direction of fibers using the engagement distribution parameters of (a) Model B, and (b) Model C estimated for each digestion time step.

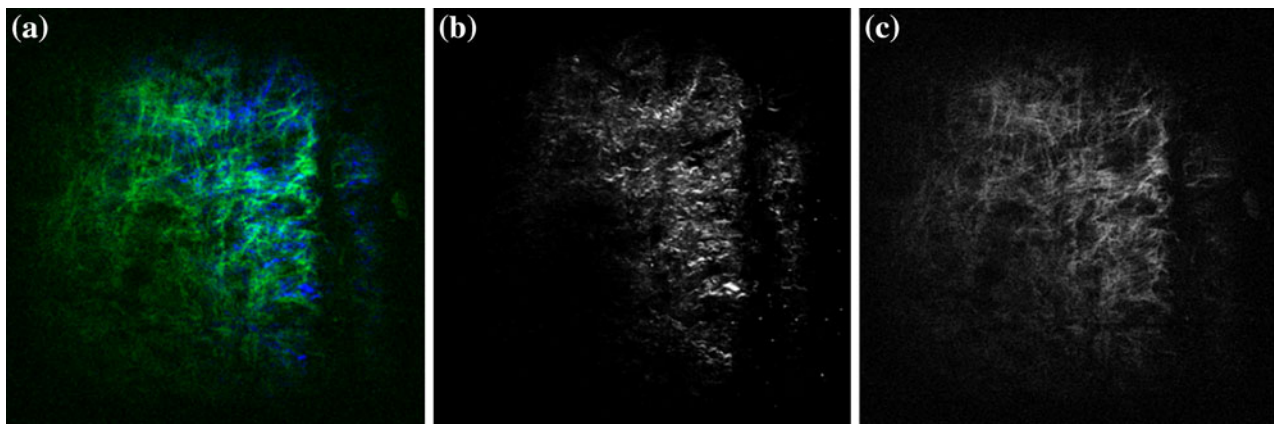


FIGURE 3. A representative microscopic image of collagen (blue) and elastin (green) captured simultaneously from the intima side of a fresh sample (a) and split into separate images of collagen (b) and elastin (c). The circumferential direction of the tissue is parallel to the horizontal edge of the images (Images are $360 \times 360 \mu\text{m}$).

the 6 and 12 h stages are significantly more undulated compared to the 24 and 48 h stages.

DISCUSSION

Elastin fibers form a resilient network that contributes to the elasticity of the arterial wall. The integrity of elastin fibers, known to have a very low turnover rate, can be compromised due to the fatigue-related damages and aging.^{3,37,48} In addition to biological impacts,^{2,6,54} loss of elastin can have direct biomechanical consequences on arteries and demands further investigations.

In this work we employed the constitutive modeling approach along with multiphoton microscopy to further elucidate the role of elastin on the arterial mechanics during a progressive *in vitro* degradation. We re-examined planar biaxial tensile test data of digested aortic tissues to estimate parameters of multiple strain energy functions previously proposed in the

literature. We showed that as elastin is digested, collagen fibers straighten out and engage earlier, describing the higher rate of stiffening and reduced extensibility. Rapid recruitment of collagen fibers seems to occur only when a large portion of elastin is degraded from the arterial tissue.

Independent studies of Ferruzzi *et al.*¹³ and Fonck *et al.*¹⁵ showed that elastin degradation dramatically increases the stiffness of mouse and rabbit carotid arteries through biaxial mechanical tests. Those studies focused on the effects of near complete loss of elastin, whereas in the current study progressive changes of the aortic tissue structure and mechanics with the gradual digestion of elastin were investigated. It is more realistic to assume that the pathologic degeneration process of elastin in diseases such as AAA occurs gradually. Consistent with the previous studies, we observed a highly coupled mechanical role for elastin and collagen using either exponential-based (Model A) or recruitment-based (Models B and C) strain energy functions. Even when the arterial wall is cut-open, the

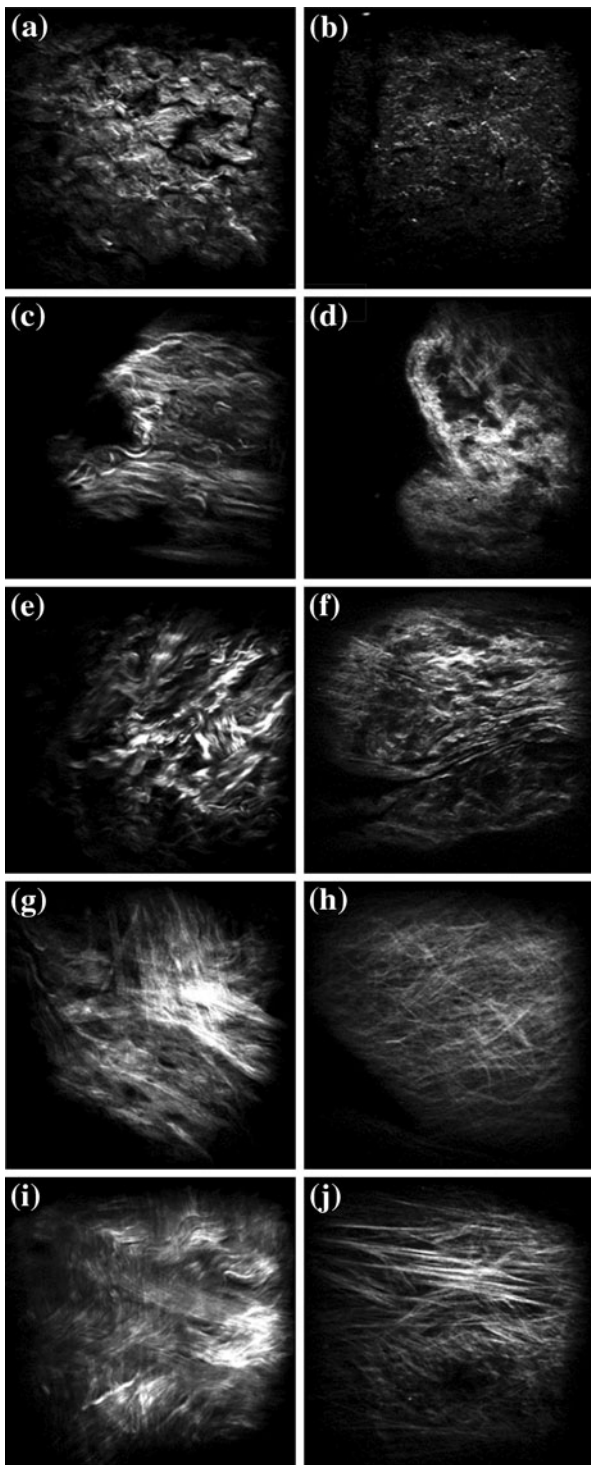


FIGURE 4. Representative microscopic images of collagen from the adventitia (*left column*) and intima (*right column*) sides at fresh (a, b), 6 h (c, d), 12 h (e, f), 24 h (g, h), and 48 h (i, j) stages. The circumferential direction of the tissue is parallel to the horizontal edge of the images (Images are $360 \times 360 \mu\text{m}$).

elastin network is pre-stretched, applying compressive forces on collagen fibers and contributing to their undulation (Fig. 4; fresh, 6, 12, and 24 h stages).

Removal of elastin reduces the undulation of fibers, resulting in an increase in the unloaded planar tissue dimensions⁹ or the diameter of arterial segments.^{10,12,13} While being less undulated in the digested tissue, collagen fibers are ready to be recruited if the tissue is loaded. It is plausible to assume that collagen fibers resist against the recoil of the stretched elastin network. In fact, Collins *et al.*¹⁰ illustrated that treatment with collagenase resulted in reduced dimensions of arteries. This is consistent with Dobrin and Canfield¹² who found a significant reduction in the tissue volume as a result of collagenase treatment.

We performed multiphoton microscopy on both the adventitia and intima sides to observe the underlying microstructural changes as a result of elastin digestion. In addition to collagen, our imaging technique allowed us to simultaneously image elastin (Fig. 3). However, elastin was no longer visible with our imaging setup after 6 h of digestion from either the adventitia or the intima side. It is therefore reasonable to suggest that what we observed from both the adventitia and intima sides (e.g., Fig. 4) is a representation of what occurs in the collagen microstructure as a result of digestion. Images of collagen in our study started to show the most noticeable change in the undulation of fibers after 24 h of degradation. Measurements of waviness for adventitial collagen also revealed that the straightness parameter reaches its maximum at 24 h (no significant change after the 24 h stage). At this stage only about 20% of original elastin content remains (Fig. 7). It appears that the presence of elastin even in small proportions contributes to the tissue elasticity and tends to keep the collagen fibers undulated. The extended toe region before the sharp stiffening behavior in the stress–stretch response at the 24 h stage further confirms this hypothesis (Fig. 1). Estimated parameters of Models A and B did not show an increasing trend in the recruitment of collagen fibers between fresh to 24 h stage despite a sharp decrease in the elastin content (Tables 1, 2, 3). After removal of the major portion of elastin, however, the engagement of collagen in load bearing was remarkably enhanced. At 6 h of digestion, there was a moderate reduction in the slope of stress–strain curves.⁹ Accordingly, a temporary reduction in collagen parameters c_1^i, c_2^i for diagonal fibers ($i = 1, 2$ in 2-fiber-family and $i = 3, 4$ in 4-fiber-family models) was anticipated by Model A. Model B also predicted a temporary delay in the engagement of fibers (i.e., increase in b_k) at the 6 h stage, contrary to the measurements results for waviness that indicate fibers are straighter at the 6 h stage compared to the non-digested condition. Originally, the circumferential direction was found to be prominently stiffer than the longitudinal direction whereas at the 24 h stage the longitudinal direction became stiffer

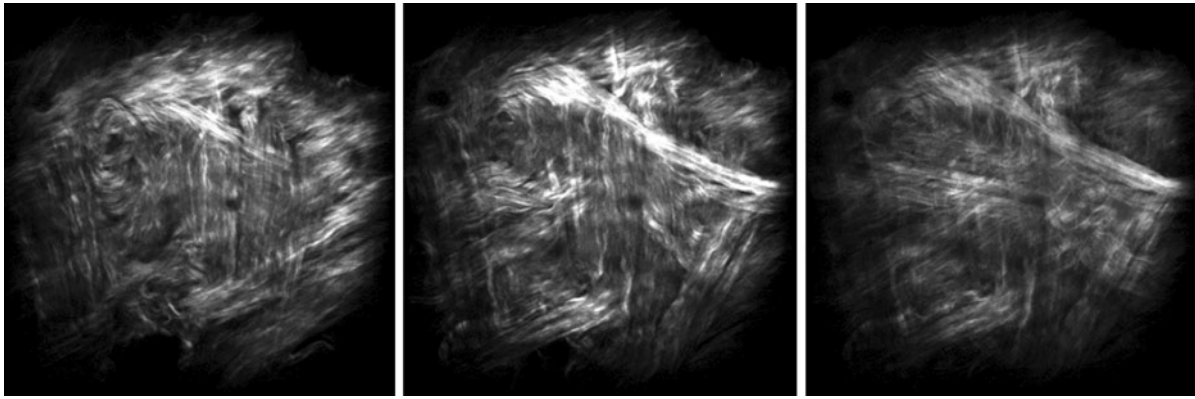


FIGURE 5. Microscopic images of collagen from the adventitia side of a sample under 48 h of elastin digestion. Images correspond to a single longitudinal and circumferential location but different scanning depth (with $6\ \mu\text{m}$ spacing). Multiple families of fibers with preferred orientations can be distinguished (Images are $360 \times 360\ \mu\text{m}$).

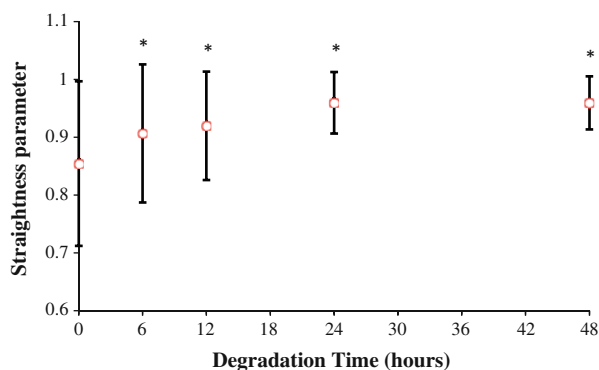


FIGURE 6. Straightness parameter (P_s) vs. degradation time. All time points are significantly greater than the fresh time point. 24 and 48 h stages are significantly greater than 6 and 12 h stages ($*p < 0.05$).

than the circumferential direction.⁹ Interestingly, at the 24 h stage, assuming mechanically identical diagonal fibers, our models also predicted $\alpha < 45^\circ$, suggesting a change in the alignment of fibers toward the longitudinal direction. However, complete digestion (after 48 or 96 h) resulted in a fairly similar mechanical response in the circumferential and longitudinal directions (i.e., $\alpha \simeq 45^\circ$ predicted by our models).

Model A presented the gradual engagement of collagen fibers with an exponential function while Models B and C considered the mechanism of engagement of collagen fibers assuming either log-logistic or normal distributions. All those models provided reasonable fits to the biaxial test data with comparable goodness of fits and were able to describe the overall behavior of arterial tissue under degradation (Fitting curves for Models B and C are not shown). Meanwhile, the engagement-based models predicted a declining trend in the parameter associated with elastin that is consistent with the reducing mass fraction.^{14,49,50} In contrast, using the exponential-based model, this

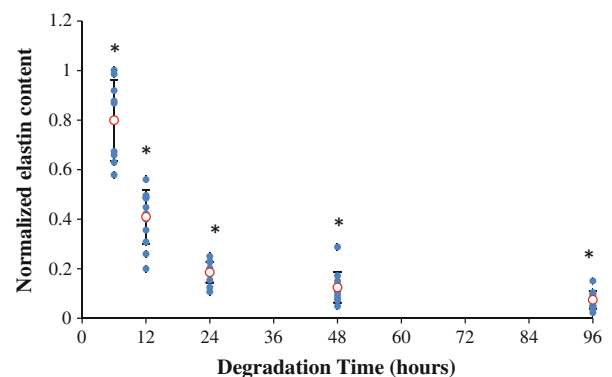


FIGURE 7. Elastin contents normalized with respect to the values at the fresh stage (0 h) vs. degradation time.⁹ All time points are significantly less than the fresh time point ($*p < 0.05$).

parameter was estimated to be almost zero in the fresh as well as the fully digested stages with no consistent trend.

Recently, Hill *et al.*²¹ quantified the gradual recruitment of collagen fibers using multiphoton microscopy while the tissues were being loaded in a uniaxial extension device. They considered a Gamma function for the distribution of recruitment stretch, similar to Sacks and Sun.⁴⁶ In a separate attempt to quantify the adventitial collagen structure, Rezakhaniha *et al.*⁴³ suggested a Beta distribution for the waviness of fibers in a zero-stress state. The measurements of waviness in our study could be used to determine the shapes of the engagement distribution density functions (as in Models B and C) at every digestion time steps. The focus of the current study, however, was not to suggest the use of a specific model that best suits vascular mechanics. Rather, it was to reflect the need for microstructural based models that are able to capture the evolving structure and mechanical properties of the arterial wall.

The multiphoton imaging in our study also revealed collagen fibers with preferred orientations, particularly, when the majority of elastin was digested and fibers became straight (Figs. 4, 5). Four major orientations for collagen fibers have been identified by Rezakhaniha *et al.*⁴³ while multi-fiber-family representation of collagen fibers has been suggested as a reasonable approximation when predicting the resulting mechanical response of arteries.^{4,14,57,58} The single fiber resolution offered by the multiphoton microscopy opens the way for the quantitative characterization of fiber dispersion and allows for a better determination of the optimal model representing the arterial wall mechanics.¹⁸ There have been many efforts to either quantify collagen fiber dispersion or include a dispersion parameter in the constitutive models to represent the distributed architecture of collagen in soft tissues.^{1,18,19,21,25,33,34,36,43,46,47}

LIMITATIONS

Non-uniqueness of best-fit parameters is an issue that arises in the nonlinear least squares estimation problems,⁴² particularly when the number of parameters in the model increases.⁵⁸ To address this concern, we have repeated the optimization process with multiple random starting points to approach global minima. The precision of the estimated parameters can be evaluated using statistical analysis such as bootstrap technique¹⁴ to provide a confidence interval for the parameters. In this work, however, we focused on the average response of multiple samples subjected to the same digestion time step, rather than estimating parameters for individual samples. The main reason for this approach is the large variability in the mechanical behavior between samples of the same group, partly due to samples having different thicknesses (1.32 ± 0.21 mm) and therefore being at a different stage of degradation considering the fixed digestion time. Ideally, we would like to perform multiple stages of digestion as well as mechanical tests on the same tissue sample to reduce the inter sample variability. However, in practice, it is difficult to perform multiple stages of chemical digestion and tensile tests on a single sample.

In addition, we considered the arterial wall as a single layer that undergoes homogenous degradation. Constitutive models considering multiple layers^{25,32} might be more appropriate as the digestion process starts from the outer layers and proceed toward the middle layer of samples.⁹ Multiphoton microscopy cannot image throughout the entire thickness of aorta which is a relatively thick artery. Imaging both sides (with 60 μ m depth from the surfaces) of the artery was

the best available approach to assess the artery structure with our experimental set up.

The role of mass fractions was considered to be inherent in the constitutive parameters. However, mass fractions could have been considered explicitly in the constitutive formulations as prescribed parameters obtained from microstructural studies.^{44,60} In addition, the assumption of isotropic response for elastin can also be regarded as a limitation of the current work since a number of studies have indicated that anisotropy of arterial elastin needs to be considered in modeling.^{1,44} In fact, recent work by Zou and Zhang⁵⁹ has demonstrated anisotropic response of arterial elastin using biaxial tensile tests. Equibiaxial mechanical testing was performed in the current work since the focus of our study was mainly on the role of elastin degradation on the evolution of tissue microstructure and mechanical properties. Non-equibiaxial tests, however, are preferred to fully characterize the highly nonlinear and anisotropic behavior of soft tissues.^{5,45,50,59} Finally, it is also noteworthy that the role of biological remodeling was overlooked in our *in vitro* tests. Aneurysms are accompanied by a remarkable cell mediated remodeling of collagen which tends to compensate the loss of elastin. Therefore, interactions between multiple constituents either through direct mechanical coupling or adaptive processes are responsible for alterations of mechanical properties in diseased arterial wall.

CONCLUSIONS

In this study we investigated progressive changes in the mechanical behavior of porcine aortic tissue under gradual elastin degradation through constitutive modeling and multiphoton imaging of the arterial wall. As a result of elastin digestion from the load-free planar samples, arterial tissues elongated in both longitudinal and circumferential directions and the collagen fibers uncoiled. An earlier and sharper recruitment as well as preferred orientations of collagen fibers was noticed in response to biaxial loads. These findings indicate an important mechanical coupling between arterial elastin and collagen and may have considerable implications in vascular mechanics and mechanobiology.

ACKNOWLEDGMENTS

This work has been supported in part by the National Heart, Lung, and Blood Institute Grant HL-098028 and National Science Foundation grants

CMMI 1100791 and CAREER 0954825. Authors would like to thank Prof. Charles P. Lin from the Wellman Center for Photomedicine for providing access to the multiphoton microscope.

REFERENCES

- ¹Agianniotis, A., R. Rezakhaniha, and N. Stergiopoulos. A structural constitutive model considering angular dispersion and waviness of collagen fibres of rabbit facial veins. *Biomed. Eng. Online* 10:18, 2011.
- ²Arribas, S. M., A. Hinek, and M. C. Gonzalez. Elastic fibres and vascular structure in hypertension. *Pharmacol. Ther.* 111:771–791, 2006.
- ³Avolio, A., D. Jones, and M. Tafazzoli-Shadpour. Quantification of alterations in structure and function of elastin in the arterial media. *Hypertension* 32:170–175, 1998.
- ⁴Baek, S., R. L. Gleason, K. R. Rajagopal, and J. D. Humphrey. Theory of small on large: potential utility in computations of fluid-solid interactions in arteries. *Comput. Methods Appl. Mech. Eng.* 196:3070–3078, 2007.
- ⁵Billiar, K. L., and M. S. Sacks. Biaxial mechanical properties of native and glutaraldehyde treated aortic valve cusps: part II—a structural constitutive model. *J. Biomech. Eng.* 122:327–335, 2000.
- ⁶Brooke, B. S., A. Bayes-Genis, and D. Y. Li. New insights into elastin and vascular disease. *Trends Cardiovasc. Med.* 13:176–181, 2003.
- ⁷Campa, J. S., R. M. Greenhalgh, and J. T. Powell. Elastin degradation in abdominal aortic aneurysms. *Atherosclerosis* 65:13–21, 1987.
- ⁸Carmo, M., L. Colombo, A. Bruno, F. R. M. Corsi, L. Roncoroni, *et al.* Alteration of elastin, collagen and their cross-links in abdominal aortic aneurysms. *Eur. J. Vasc. Endovasc. Surg.* 23:543–549, 2002.
- ⁹Chow, M. J., J. R. Mondonedo, V. M. Johnson, and Y. Zhang. Progressive structural and biomechanical changes in elastin degraded aorta. *Biomech. Model. Mechanobiol.* 2013 (in print).
- ¹⁰Collins, M. J., J. F. Eberth, E. Wilson, and J. D. Humphrey. Acute mechanical effects of elastase on the infrarenal mouse aorta: implications for models of aneurysms. *J. Biomech.* 45:660–665, 2012.
- ¹¹Dobrin, P. B., W. H. Baker, and W. C. Gley. Elastolytic and collagenolytic studies of arteries. *Arch. Surg.* 119:405–409, 1984.
- ¹²Dobrin, P. B., and T. R. Canfield. Elastase, collagenase, and the biaxial elastic properties of dog carotid artery. *Am. J. Physiol.* 247:H124–H131, 1984.
- ¹³Ferruzzi, J., M. J. Collins, A. T. Yeh, and J. D. Humphrey. Mechanical assessment of elastin integrity in fibrillin-1-deficient carotid arteries: implications for Marfan syndrome. *Cardiovasc. Res.* 92:287–295, 2011.
- ¹⁴Ferruzzi, J., D. A. Vorp, and J. D. Humphrey. On constitutive descriptors of the biaxial mechanical behavior of human abdominal aorta and aneurysms. *J. R. Soc. Interface* 8:435–450, 2011.
- ¹⁵Fonck E., G. Prod'hom, S. Roy, L. Augsburg, D. A. Rufenacht, and N. Stergiopoulos. Effect of elastin degradation on carotid wall mechanics as assessed by a constituent-based biomechanical model. *Am. J. Physiol. Heart. Circ. Physiol.* 292:H2754–H2763, 2007.
- ¹⁶Fung, Y. C. Elasticity of soft tissues in simple elongation. *Am. J. Physiol.* 213:1532–1544, 1967.
- ¹⁷Fung, Y. C., K. Fronek, and P. Patitucci. Pseudoelasticity of arteries and the choice of its mathematical expression. *Am. J. Physiol.* 237:H620–H631, 1979.
- ¹⁸Gasser, T. C., R. W. Ogden, and G. A. Holzapfel. Hyperelastic modelling of arterial layers with distributed collagen fibre orientations. *J. R. Soc. Interface* 3:15–35, 2006.
- ¹⁹Haskett D., G. Johnson, A. Zhou, U. Utzinger, J. Vande Geest. Microstructural and biomechanical alterations of the human aorta as a function of age and location. *Biomech. Model. Mechanobiol.* 9:725–736, 2010.
- ²⁰He, C. M., and M. R. Roach. The composition and mechanical properties of abdominal aortic aneurysms. *J. Vasc. Surg.* 20:6–13, 1994.
- ²¹Hill, M. R., X. Duan, G. A. Gibson, S. Watkins, and A. M. Robertson. A theoretical and non-destructive experimental approach for direct inclusion of measured collagen orientation and recruitment into mechanical models of the artery wall. *J. Biomech.* 45:762–771, 2012.
- ²²Holzapfel, G. A. *Nonlinear Solid Mechanics: A Continuum Approach for Engineering*. New York: Wiley, 2000.
- ²³Holzapfel, G. A., T. C. Gasser, and R. W. Ogden. A new constitutive framework for arterial wall mechanics and a comparative study of material models. *J. Elasticity* 61:1–48, 2000.
- ²⁴Holzapfel, G. A., and R. W. Ogden. Constitutive modelling of arteries. *Proc. R. Soc. A* 466:1551–1597, 2010.
- ²⁵Holzapfel, G. A., G. Sommer, T. C. Gasser, and P. Regitnig. Determination of the layer-specific mechanical properties of human coronary arteries with non-atherosclerotic intimal thickening, and related constitutive modelling. *Am. J. Physiol. Heart Circ. Physiol.* 289:H2048–H2058, 2005.
- ²⁶Holzapfel, G. A., and H. W. Weizsacker. Biomechanical behavior of the arterial wall and its numerical characterization. *Comput. Biol. Med.* 28:377–392, 1998.
- ²⁷Humphrey, J. D. Remodeling of a collagenous tissue at fixed lengths. *J. Biomech. Eng.* 121:591–597, 1999.
- ²⁸Humphrey, J. D. *Cardiovascular Solid Mechanics; Cells, Tissues, and Organs*. New York: Springer, 2002.
- ²⁹Humphrey, J. D. Continuum biomechanics of soft biological tissues. *Proc. R. Soc. A* 459:3–46, 2003.
- ³⁰Humphrey, J. D., and G. A. Holzapfel. Mechanics, mechanobiology, and modeling of human abdominal aorta and aneurysms. *J. Biomech.* 45:805–814, 2012.
- ³¹Humphrey, J. D., and C. A. Taylor. Intracranial and abdominal aortic aneurysms: similarities, differences, and need for a new class of computational models. *Annu. Rev. Biomed. Eng.* 10:221–246, 2008.
- ³²Kroon, M., and G. A. Holzapfel. A new constitutive model for multi-layered collagenous tissues. *J. Biomech.* 41:2766–2771, 2008.
- ³³Lanir, Y. A structural theory for the homogeneous biaxial stress-strain relationships in flat collagenous tissues. *J. Biomech.* 12:423–436, 1979.
- ³⁴Lanir, Y. Constitutive equations for fibrous connective tissues. *J. Biomech.* 16:1–12, 1983.
- ³⁵Lindeman, J. H. N., B. A. Ashcroft, J. M. Beenakker, M. vanEs, N. B. R. Koekkoek, F. A. Prins, J. F. Tieleman, H. Abdul-Hussien, R. A. Bank, and T. H. Oosterkamp. Distinct defects in collagen microarchitecture underlie vessel-wall failure in advanced abdominal aneurysms and

- aneurysms in Marfan syndrome. *Proc. Natl. Acad. Sci.* 107:862–865, 2010.
- ³⁶Lokshin, O., and Y. Lanir. Micro and macro rheology of planar tissues. *Biomaterials* 30:3118–3127, 2009.
- ³⁷Marque, V., P. Kieffer, B. Gayraud, I. Lartaud-Idjouadiene, F. Ramirez, and J. Atkinson. Aortic wall mechanics and composition in a transgenic mouse model of Marfan syndrome. *Arterioscler. Thromb. Vasc. Biol.* 21:1184–1189, 2001.
- ³⁸Meijering, E. Neuron tracing in perspective. *Cytometry A* 77:693–704, 2010.
- ³⁹Meijering, E., M. Jacob, J. C. Sarria, P. Steiner, H. Hirling, and M. Unser. Design and validation of a tool for neurite tracing and analysis in fluorescence microscopy images. *Cytometry A* 58:167–176, 2004.
- ⁴⁰Menashi, S., J. S. Campa, R. M. Greenhalgh, and J. T. Powell. Collagen in abdominal aortic-aneurysm—typing content, and degradation. *J. Vasc. Surg.* 6:578–582, 1987.
- ⁴¹Mouton, P. R. Principles and practices of unbiased stereology. Baltimore: The Johns Hopkins University Press, 2002.
- ⁴²Ogden, R. W., G. Saccomandi, and I. Sgura. Fitting hyperelastic models to experimental data. *Comput. Mech.* 34:484–502, 2004.
- ⁴³Rezakhaniha, R., A. Agianniotis, J. T. C. Schrauwen, A. Griffa, D. Sage, C. V. C. Bouten, F. N. van de Vosse, M. Unser, and N. Stergiopoulos. Experimental investigation of collagen waviness and orientation in the arterial adventitia using confocal laser scanning microscopy. *Biomech. Model. Mechanobiol.* 11:461–473, 2012.
- ⁴⁴Rezakhaniha, R., E. Fonck, C. Genoud, and N. Stergiopoulos. Role of elastin anisotropy in structural strain energy functions of arterial tissue. *Biomech. Model. Mechanobiol.* 10:599–611, 2011.
- ⁴⁵Sacks, M. S. Biaxial mechanical evaluation of planar biological materials. *J. Elast.* 61:199–246, 2000.
- ⁴⁶Sacks, M. S., and W. Sun. Multiaxial mechanical behavior of biological materials. *Annu. Rev. Biomed. Eng.* 5:251–284, 2003.
- ⁴⁷Schriebl, A. J., G. Zeindlinger, D. M. Pierce, P. Regitnig, and G. A. Holzapfel. Determination of the layer-specific distributed collagen fibre orientations in human thoracic and abdominal aortas and common iliac arteries. *J. R. Soc. Interface* 9:1275–1286, 2012.
- ⁴⁸Tsamis, A., A. Rachev, and N. Stergiopoulos. A constituent-based model of age-related changes in conduit arteries. *Am. J. Physiol. Heart Circ. Physiol.* 301:H1286–H1301, 2011.
- ⁴⁹Vande Geest, J. P., M. S. Sacks, and D. A. Vorp. Age dependency of the biaxial biomechanical behavior of human abdominal aorta. *J. Biomech. Eng.* 126:815–822, 2004.
- ⁵⁰Vande Geest, J. P., M. S. Sacks, and D. A. Vorp. The effects of aneurysm on the biaxial mechanical behavior of human abdominal aorta. *J. Biomech.* 39:1324–1334, 2006.
- ⁵¹Veilleux, I., J. A. Spencer, D. P. Biss, and C. P. Lin. In vivo cell tracking with video rate multimodality laser scanning microscopy. *IEEE J. Sel. Top. Quantum Electron.* 14:10–18, 2008.
- ⁵²Vorp, D. A. Biomechanics of abdominal aortic aneurysm. *J. Biomech.* 40:1887–1902, 2007.
- ⁵³Vorp, D. A., and J. P. Vande Geest. Biomechanical determinants of abdominal aortic aneurysm rupture. *Arterioscler. Thromb. Vasc. Biol.* 25:1558–1566, 2005.
- ⁵⁴Wachi, H. Role of elastic fibers on cardiovascular disease. *J. Health Sci.* 57:449–457, 2011.
- ⁵⁵Wagner, H. P., and J. D. Humphrey. Differential passive and active biaxial mechanical behaviors of muscular and elastic arteries: basilar versus common carotid. *J. Biomech. Eng.* 133:051009, 2011.
- ⁵⁶Watton, P. N., V. Yiannis, and G. A. Holzapfel. Modelling the mechanical response of elastin for arterial tissue. *J. Biomech.* 42:1320–1325, 2009.
- ⁵⁷Wicker, B. K., H. P. Hutchens, Q. Wu, A. T. Yeh, and J. D. Humphrey. Normal basilar artery structure and biaxial mechanical behaviour. *Comput. Methods Biomech. Biomed. Eng.* 11:539–551, 2008.
- ⁵⁸Zeinali-Davarani, S., J. Choi, and S. Baek. On parameter estimation for biaxial mechanical behavior of arteries. *J. Biomech.* 42:524–530, 2009.
- ⁵⁹Zou, Y., and Y. Zhang. An experimental and theoretical study on the anisotropy of elastin network. *Ann. Biomed. Eng.* 37:1572–1583, 2009.
- ⁶⁰Zulliger, M. A., P. Frideza, K. Hayashi, and N. Stergiopoulos. A strain energy function for arteries accounting for wall composition and structure. *J. Biomech.* 37:989–1000, 2004.